DETECTION OF JETS AND ASSOCIATED TOROIDAL FIELDS IN THE SOLAR TACHOCLINE

Jørgen Christensen-Dalsgaard[1,2], **Thierry Corbard**[3], **Mausumi Dikpati**[2], **Peter A. Gilman**[2], **and Michael J. Thompson**[4,2]

[1] *Department of Physics and Astronomy, University of Aarhus, DK-8000, Aarhus C, Denmark*

[2] *High Altitude Observatory, National Center for Atmospheric Research, 3450 Mitchell Lane, Boulder CO 80301, USA*

[3] *Observatoire de la Côte d'Azur, Laboratoire Cassiopée, B.P. 4229, F-06304, Nice, France*

[4] *Space & Atmospheric Physics Group, The Blackett Laboratory, Imperial College, London SW7 2BW, UK*

ABSTRACT

Tachocline toroidal fields are likely to exist in the form of narrow bands, at least during some phases of the solar cycle. Recent theoretical studies show that a narrow toroidal band in the solar tachocline can be held in equilibrium against its poleward slip due to the curvature stress by Coriolis forces from a prograde jet inside the band. Early attempts to detect convection-zone jets were made with the 7-month GONG data available at that time, but no clear evidence of jets was detected. We explore here long-term GONG data, in order to detect the amplitude, width and the latitude-location of jets that could exist in addition to background zonal flows. Using the latitudinal force-balance equation for toroidal bands in a typical solar tachocline, we first generate artificial helioseismic data that contain jets and we invert them in order to recover the jets. After this validation of the technique, we apply it to inversion of real data at different epochs.

Key words: solar dynamo; Sun: tachocline.

1. INTRODUCTION AND MOTIVATION

The solar tachocline, a thin layer (of $< 0.05R$ thickness) located at or below the base of the convection zone, contains a strong radial differential rotation, and hence is the place where strong toroidal magnetic fields are most likely to be generated by a dynamo process.

In order for toroidal fluxtubes to achieve 100 kG strength through the amplification by the dynamo process, those fluxtubes need to be stored in the tachocline for a sufficiently long time. Two different processes can lead to destabilization and the loss of equilibrium of these fluxtubes in the tachocline; (i) the escape towards the surface due to their magnetic buoyancy (Parker 1979), and (ii) the poleward slip due to their curvature stress (Spruit and van Ballegooijen 1982).

While subadiabatic stratification in the tachocline provides some storage against their buoyant escape through the convection zone, to balance the poleward curvature stress either one or both of the following two mechanisms are necessary: (i) an equatorward hydrostatic pressure gradient created by piling up mass on the poleward side of the toroidal band; and (ii) an equatorward Coriolis force created by a prograde jet developed in the toroidal band (Dikpati and Gilman 2001; Rempel, Schüssler and Tóth 2000). Rempel and Dikpati (2003) have further shown that the approach of Dikpati and Gilman (2001) can be considered as a first-order approximation of the approach of Rempel et al. (2000). More generally, a toroidal band can be held against its poleward slip by the combination of a jet-like flow inside the band and a mass pile-up on the poleward side of the band. When the jet is only partly responsible for holding the toroidal band against its poleward slip, we refer to such a jet as 'fractional'.

Cally, Dikpati and Gilman (2004) showed in a nonlinear evolution of the 2D MHD tachocline instabilities that the tachocline latitudinal differential rotation achieves a plausible equilibrium state by forming a fractional jet, for example a $\sim 20\%$ jet for a $10°$ band placed at $40°$ latitude.

The prolateness estimate of Charbonneau et al. (1999a) is consistent with toroidal fields of 60-150 kGauss, if the field were held in equilibrium in the overshoot tachocline purely by mass pile-up; whereas the jet estimate of Rempel et al. (2000) indicates that a 200 $\mathrm{m\,s^{-1}}$ prograde jet can create force-balance for a 100 kGauss toroidal band. Therefore, helioseismic estimation of both the prolateness of the tachocline as well as the jet amplitude are necessary to determine the strength of the tachocline toroidal bands. We can only obtain a lower limit of the toroidal field if we determine the field strength from an estimate of one of these two.

It is to be noted that, apart from such a prograde jet inside a toroidal band, there could be submerged polar jets of hydrodynamic origin. Charbonneau, Dikpati and Gilman (1999b) showed, in a purely hydrodynamic stability analysis of the solar latitudinal differential rotation, that the angular momentum transport by the Reynolds stress associated with the growing perturbation flow should lead to localized spin-up at high latitudes. Similar features were also noted in SOI-MDI data (Schou et al. 1998; Howe et al. 1998).

2. RELATION BETWEEN THE JET AND TOROIDAL FIELD

We use expression (3) of Rempel and Dikpati (2003) in order to produce artificial data for a tachocline jet associated with a toroidal band there. Thus we specify the strengh of the jetlike flow, expressed as an angular frequency, as

$$\omega_{\rm j} = \sqrt{\left(\omega_{\rm c} + \omega_{\rm s}\right)^2 + (1-\varepsilon)\ \alpha_0^2} - \left(\omega_{\rm c} + \omega_{\rm s}\right). \qquad (1)$$

Here $\omega_{\rm j}$ is the jetlike toroidal flow, $\omega_{\rm c}$ is the core rotation rate, $\omega_{\rm s}$ is the solar-like differential rotation, ε is the jet parameter, and $\alpha_0\left(1-\mu^2\right)^{1/2}$ is the toroidal field. Note that ε can vary between 1 (no jet) and 0 (full jet). In reality, ε might have a value less than 1, which would denote a fractional (ϵ) jet.

We prescribe a Gaussian-type profile in latitude (Dikpati and Gilman 1999) and the following radial profile $f(r)$ for the toroidal band in the solar tachocline of thickness $0.05R$:

$$f(r) = \frac{1}{2}\left\{1+\mathrm{erf}\left(\frac{r-0.675R}{0.02R}\right)\right\} \qquad (2)$$

$$\times\frac{1}{2}\left\{1-\mathrm{erf}\left(\frac{r-0.725R}{0.02R}\right)\right\}. \qquad (3)$$

The strength of the jet, as a function of magnetic field strength, is shown in Fig. 1.

In order to simulate data similar to those used in helioseismic inversions for the Sun, the jet is embedded in a background rotation profile that is similar to the solar internal rotation inferred by helioseismology. The background we use has solar-like latitudinal differential in the convection zone (outer 30 per cent of the solar radius) and a tachocline-like transition to uniform rotation in the radiative interior. The jet profile for a 10° band is illustrated in Fig. 2, both on its own and when added to the background rotation profile. The magnetic band associated with the jet has been placed at four different latitudes. The corresponding combined profiles for a 20° jet are shown in Fig. 3.

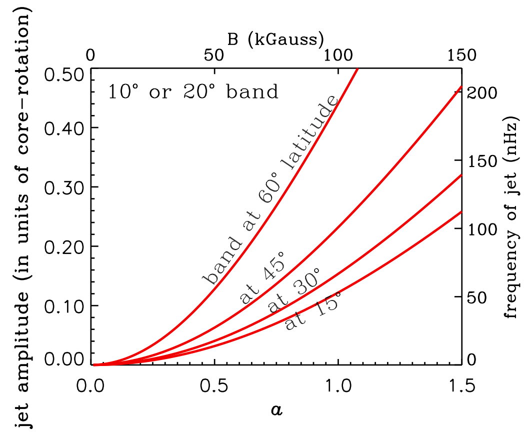

Figure 1. Jet amplitude as a function of peak field strength of a toroidal band placed at different latitudes.

3. INVERSION TECHNIQUE AND RESULTS WITH ARTIFICIAL DATA

Christensen-Dalsgaard et al. (1998) attempted to detect convection-zone jets with the 7-month GONG data available at that time. In their experiments with artificial data, Christensen-Dalsgaard et al. resolved a jet of 40 nHz contrast in the lower convection zone. But no real jet was found from this dataset. Now we have access to data over much longer time base. We are applying the 2D Regularised Least-Squares (RLS) inversion technique with improved averaging kernel to search for tachocline jets and analyze their properties in order to explore the toroidal field features there.

The method is calibrated by reproducing the jet obtained from the inversion of the artificial data. In all cases the jet is such as to balance fully ($\epsilon = 1$) a 20°-wide toroidal magnetic band with peak field strength of 60 kG. The signature of such a jet in the inversion is quite subtle, the solutions with jets looking superficially very similar to those with no jet (see Fig. 4). However, when the difference is taken between the solution with jet and the solution without jet, the presence of the jet is very clear. So as to study the effects of resolution without confusion, we have not employed different noise realizations in the two solutions being differenced. However, the amplitude of the recovered jet, although reduced from the amplitude of the original jet used to create the splittings data, is in all cases above the level of the errors. If the jet strength were to be greater by a factor of 4, say, the jet would be clear even in the un-differenced solution (Fig. 4).

We also note that a narrower jet is harder to detect: for example, to detect reliably the jet inside a 10°-band in force-balance, a larger amplitude of artificial jet data, such as produced by a 120 kG peak field, is necessary.

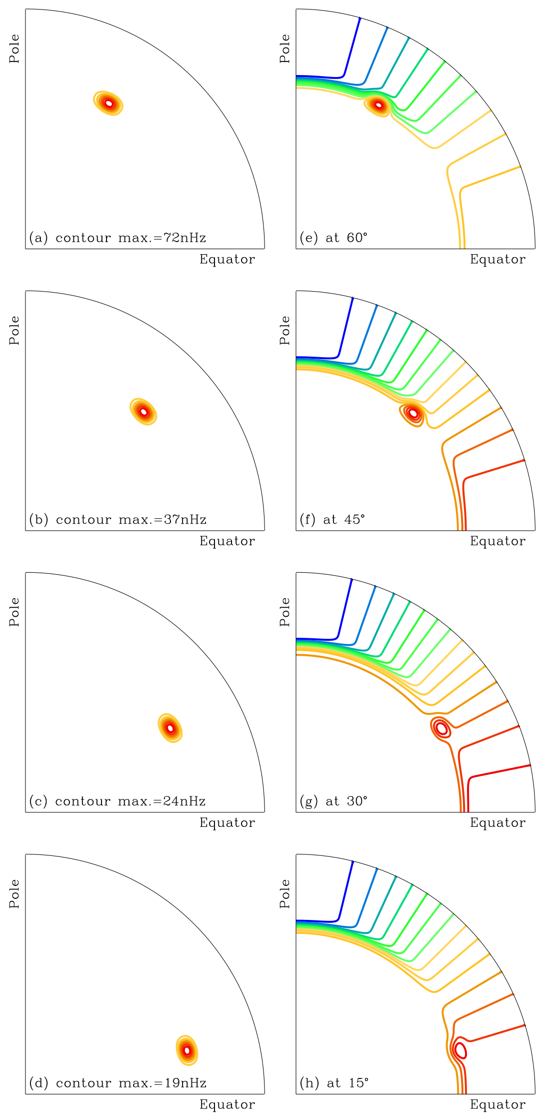

Figure 2. Jet and total internal rotation including background for a 10° *band with 60 kG peak field, assuming that balance is entirely between magnetic curvature stress and Coriolis force.*

4. RESULTS WITH REAL DATA

As the artificial data experiments indicate that the jets show up best when differencing inversions, we separately inverted 108-day GONG data and differenced the results. Fig. 5 shows the inversions of data for GONG months 74-76 (17 July - 2 Nov. 2002) and for GONG months 69-71 (18 Jan. - 5 May 5 2002) and their difference. The differences show quite a prominent jet-like signature at about 60 degrees near the tachocline!

We have inverted and differenced other 108-day GONG datasets. Some of these are illustrated in Fig. 6: in each case the particular period of 3 GONG months is indicated, and the results have been differenced with the average rotation over all eight epochs. Caution is required,

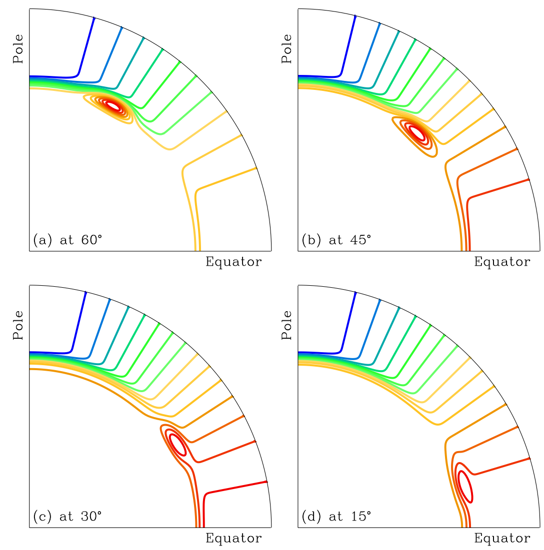

Figure 3. As Fig. 2 but for a wider, 20° *band of magnetic field.*

as data noise can produce differences purely due to noise, and spatial correlations between neighbouring points in the plane can then create jet-like artifacts particularly where the error is largest, in the core and near the polar axis. We point out, however, (see panels in the right column of Fig. 6) a jet-like feature that appears to migrate equatorward from GONG month 36 (at 60°) to GONG month 46 (at 45°, about one year later) to GONG month 56 (at 30°, about two years later).

We expect a prograde jet associated with a band of strong toroidal field to be found underneath the surface latitudes where sunspots are seen. Therefore it is unclear what relation exists between the jets seen at 60° and 45° (lower-left panel of Fig. 5 and the two upper-right panels of Fig. 6) and the toroidal field. Could high-latitude jets instead have their origins in the global hydrodynamic instability of the solar latitudinal differential rotation (Charbonneau et al. 1999b)? As a next step we shall look at differences between one-year averages at solar minimum and solar maximum, which will have smaller errors.

The bottom left panel in Fig. 6 shows the inversion for GONG months 85-87 (108 days from 17 Aug. to 2 Dec. 2003), a time during which both north and south hemispheres display large sunspots at very low latitudes and large flares went off. Unfortunately we do not see low-latitude jets near the tachocline. We speculate that this may be because a toroidal band close to the equator needs little or no jet (see Fig. 2) for the force-balance. If this is the explanation, then we might see the systematic decrease in the jet amplitude if the jet associated with a toroidal band is detected at successively lower latitudes with the progress of the solar cycle.

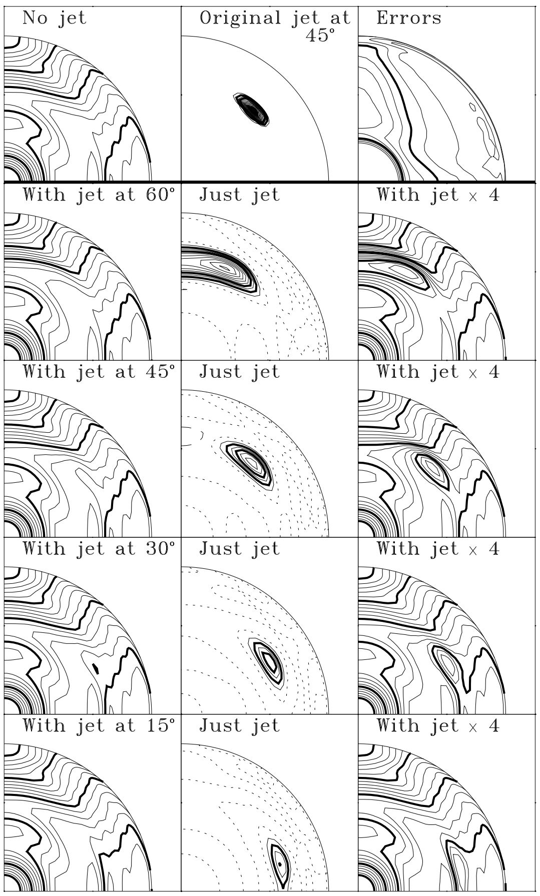

Figure 4. Top row: top left panel shows the inversion of jet-free artificial data; top center panel shows a jet (without any inversion) arising from a 20° band at 45° latitude for comparison with the width and strength of the features in the panels beneath it; top right panel shows the formal errors on the inversions. Each subsequent row shows the inversion experiment for a differently located jet, as indicated: the first column shows inversion of data with the jet included; the second column shows the difference between the previous inversion and the inversion with no jet present (as in top left panel); the third column shows the inversion with the jet enhanced by factor 4. The full inversions have contours every 10 nHz, with contours at 300 nHz (near pole), 350 nHz, 400 nHz and 450 nHz bold. The panels in column 2 show contours every 2 nHz, with the 4 nHz and 8 nHz contours bold; the zero contour is shown dotted. The error contours (top right panel) are at 1 nHz spacings, with the 4 nHz and 8 nHz contours shown bold; errors increase with depth.

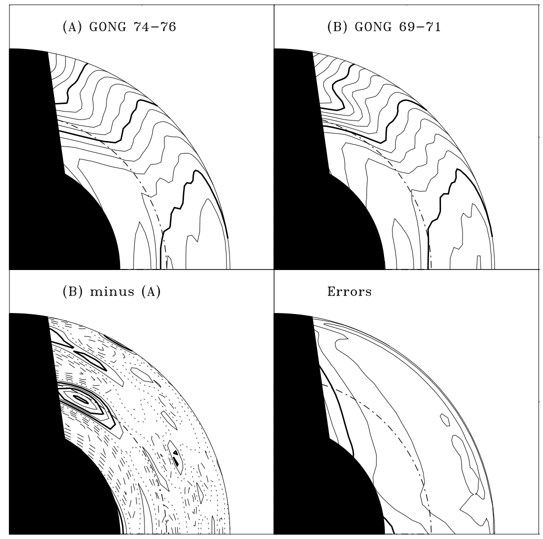

Figure 5. Inversions of 108-day GONG splittings data for GONG months 74-76 (17 July - 2 Nov. 2002) and for GONG months 69-71 (18 Jan. - 5 May 2002) and their differences.

ACKNOWLEDGMENTS

We thank Rachel Howe for her help in making the GONG splittings data available to us. This work utilizes data from the Global Oscillations Network Group (GONG). The GONG project is supported by the National Science Foundation (NSF) and is carried out by the National Solar Observatory, Tucson, Arizona under AURA. M.D. acknowledges support from NASA through awards W-10107 & W-10175. National Center for Atmospheric Research is sponsored by National Science Foundation.

REFERENCES

Cally P. S., Dikpati M., and Gilman P. A. *Highlights of Astronomy, IAU 2003*, ed. O. Engvold, in the press, 2004.

Christensen-Dalsgaard J., Howe R., Schou J., Thompson M. J. and Toomre J. Can convection-zone jets be detected with GONG 7-month data?, in *Sounding Solar & Stellar Interior*, IAU Symposium 181, Poster vol., Observatoire de Nice, 165 – 166, 1998.

Charbonneau P., et al. Helioseismic constraints on the structure of the solar tachocline, *Astrophysical Journal*, Vol. 527, 445 – 460, 1999a.

Charbonneau P., Dikpati M., and Gilman P. A. Stability of the solar latitudinal differential rotation inferred from helioseismic data, *Astrophysical Journal*, Vol. 526, 523 – 537, 1999b.

Dikpati M. and Gilman P. A. Joint instability of latitudinal differential rotation and concentrated toroidal fields below the solar convection zone, *Astrophysical Journal*, Vol. 512, 417 – 441, 1999.

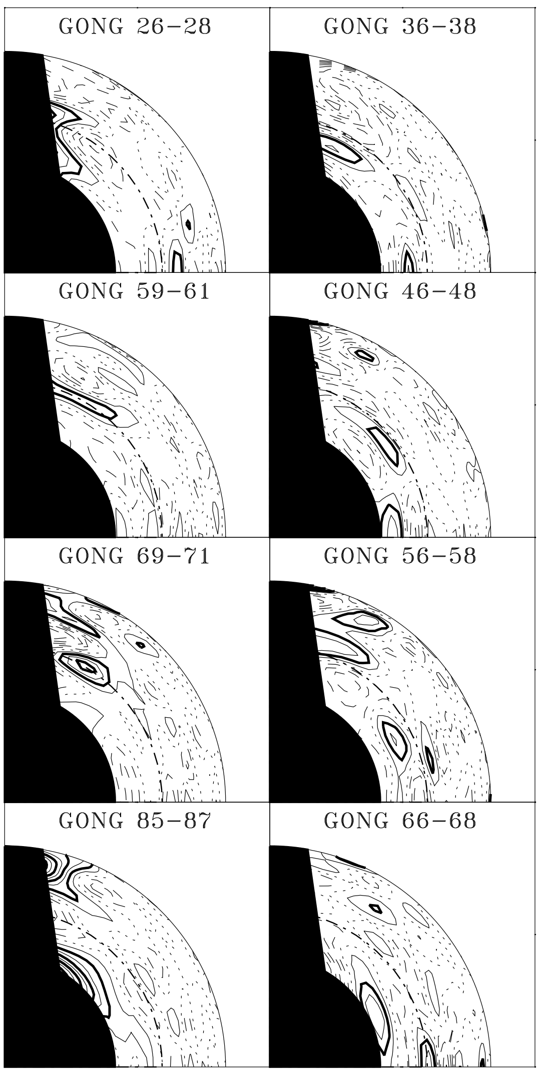

Figure 6. Inversions of various 108-day GONG splittings datasets, differenced with the mean of all eight sets.

Dikpati M. and Gilman P. A. Prolateness of the solar tachocline inferred from latitudinal force balance in a magnetohydrodynamic shallow-water model, *Astrophysical Journal*, Vol. 552, 348 – 353, 2001.

Howe R., et al. The SOI-MDI high-latitude jet: the evidence for and against, *Structure and Dynamics of the Interior of the Sun and Sun-like Stars, ESA-SP 418*, 803 – 808, 1998.

Parker E. N., *Cosmical Magnetic Fields; their origin and their activity*, Oxford University Press, 1979.

Rempel M. and Dikpati M. Storage and equilibrium of toroidal magnetic fields in the solar tachocline: a comparison between MHD shallow-water and full MHD approaches, *Astrophysical Journal*, Vol. 584, 524 – 527, 2003.

Rempel M., Schüssler M., and Tóth G. Storage of magentic flux at the bottom of the solar convection zone, *Astronomy and Astrophysics*, Vol. 363, 789 – 799, 2000.

Schou J., et al. Helioseismic studies of differential rotation in the solar envelope by the Solar Oscillations Investigation using the Michelson Doppler Imager, *Astrophysical Journal*, Vol. 505, 390 – 417, 1998.

Spruit H. C. and van Ballegooijen A. A. Stability of toroidal flux tubes in stars, *Astronomy and Astrophysics*, Vol. 106, 58 – 66 (Erratum: *Astronomy and Astrophysics*, Vol. 350, 113), 1982.